Proceedings of the 5th International Conference of Fluid Flow, Heat and Mass Transfer (FFHMT'18)
Niagara Falls, Canada – June 7 – 9, 2018
Paper No. 135
DOI: 10.11159/ffhmt18.135

Numerical Investigation on the Effects of Operating Conditions on the Performance of a Steam Jet-Ejector

Seyedali Sabzpoushan[1], Masoud Darbandi[1], Gerry E. Schneider[2]
[1]Center of Excellence in Aerospace Systems, Department of Aerospace Engineering, Sharif University of Technology
Azadi Ave., P. O. Box 11365-8639, Tehran, Iran
s_sabzpoushan@ae.sharif.edu; darbandi@sharif.edu
[2]Department of Mechanical and Mechatronics Engineering, University of Waterloo
Waterloo, Ontario, N2L 3G1, Canada
gerry.schneider@uwaterloo.ca

Abstract - In this paper, the focus is on an existing steam jet-ejector, in which the primary flow is high pressure superheated steam and the suction flow is a mixture of saturated steam and air. The main goal of this work is to improve the ejector performance via proper setting of its working conditions such as setting motive, suction and discharge pressures and even primary and secondary streams composition, albeit if it is possible. From the computational perspective, the modelling and simulation of fluid flow are very complicated in an ejector because of facing with simultaneous subsonic and supersonic regimes, very high and very low pressure regions close to each other inside the ejector, complex turbulent mixing, and imperative heat transfer conditions. This study aims to improve the entrainment ratio of the existing steam jet-ejector by investigating its performance under different operating conditions and reduce the consumption of motive steam, which is a critical issue in the current human society because of facing with major global warming and water crisis conditions. The results show that by lowering the motive pressure, the achieved entrainment ratio increases up to 51% percent, while the ejector critical back pressure decreases. Obeying the current strategy, the annual water consumption of the vacuum system can be reduced about 3000 m^3 in the current combined power cycle unit.

Keywords**:** Ejector, Vacuum, Steam, Suction, Entrainment Ratio, Turbulent Mixing, Isentropic Expansion.

1. Introduction

Ejector is a device for compressing or entraining fluid flows or even solid particles. Ejector has no moving part and uses the potential of a high pressure flow to suck and compress a low pressure flow. Figure 1 presents the main parts of an ejector including primary nozzle, secondary inlet, suction and mixing chambers, secondary throat, and exit diffuser. The current target ejector is a steam ejector, which is used as the vacuum system of an air-cooled condenser (ACC) of the steam turbine in a combined thermal power cycle and has the duty to evacuate the remaining steam and non-condensable gases from the heat exchangers.

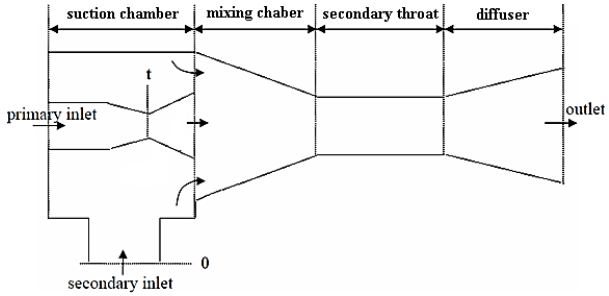

Fig. 1: Main parts of an ejector [1].

Ejectors can be categorized based on the direction of the primary and secondary flows entering to the ejector including axial-axial and axial-radial flow ejectors. The current ejector, which is of type of axial-radial flow, has the duty of sucking a mixture of 62.5 kg/hr of saturated steam and 25 kg/hr of air at pressure of 24.5 kPa, abs. (steam turbine design back

pressure) and discharging them into an ambient with pressure and temperature of about 35.5 kPa (abs.) and 106.9 ^{o}C. Because of the radial entrance of the secondary stream, the existing ejector has a low entrainment ratio (ER) of about 16 percent and consumes 545 kg/hr superheated motive steam at pressure and temperature of 17.3 bar (abs.) and 445 ^{o}C. Due to the low performance of current in-service ejector, it has been replaced by an axial-axial flow ejector for the current performance studies. This alternative ejector, which is shown schematically in Figure 2, has the entrainment ratio of about 40 percent at the aforementioned operating condition, i.e., the design point.

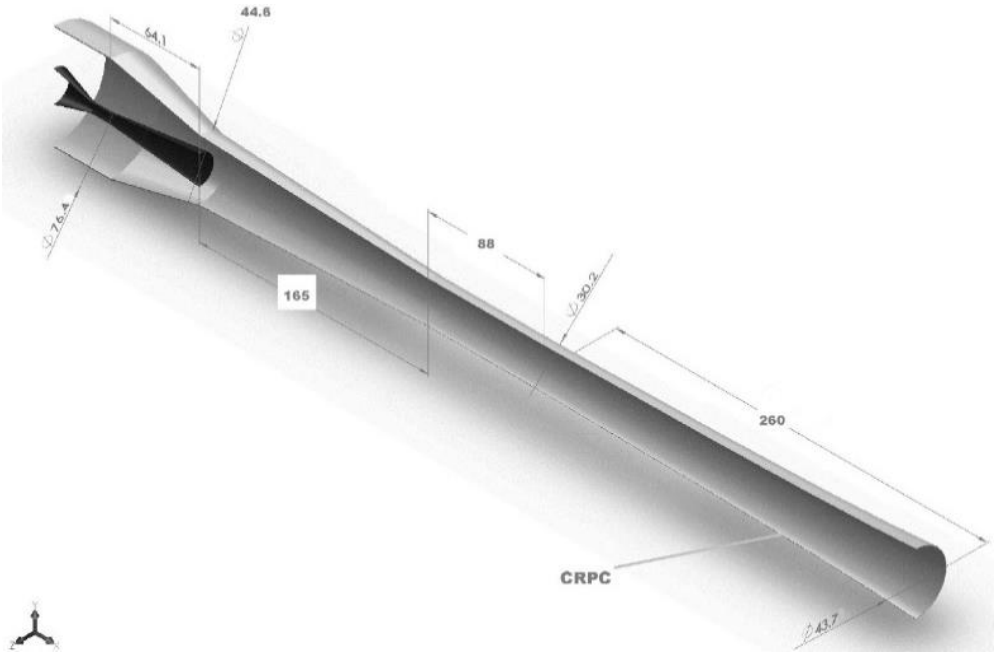

Fig. 2: Isometric view of the simulated geometry.

The past numerical efforts on simulation and performance improvement of ejectors found in literature are presented partly here. Riffat et al. [2] numerically solved an ejector in a refrigeration cycle using three different working fluids and three motive nozzle configurations. Kim et al. [3] also simulated compressible flow field inside an ejector in 2D axisymmetric space. In a numerical-experimental research, Al-Ansary et al. [4] proposed a performance study on a single phase air-air ejector using the $RNG\ k-\varepsilon$ turbulence model. One of the 3D simulations found in literature proposed by Alhussan and Garris [5], in which unsteady operation of an ejector was investigated. In literature, there have been other scholars that investigated the effect of some geometrical and operating parameters on the performance of ejectors in general [6, 7]. Watanawanavet [8] studied the effect of the primary nozzle area ratio on the suction performance, and Zhang et al. [9] and Varga et al. [10] proposed the use of an oval body in the primary throat to adjust the desired motive mass flow in different working conditions. An intensive study on the effect of the geometrical features of the primary nozzle on the ejector performance has been proposed by Fu et al. [11]. For optimization efforts on the mixing chamber geometry, it could be pointed to the research published by Palacz et al. [12]. Some scholars paid attention to changing the pressure and temperature operating conditions of ejectors with axial-radial [14] or axial-axial [15] flows. Composition of the inlet streams, e.g. air mass fraction in the suction flow, could be influential to the suction capacity of ejector. This aspect has been investigated by Shafaee et al. [16]. A more comprehensive research could be study the simultaneous effect of the geometrical parameters and operating conditions, which proposed by Jeong et al. [17] using ideal gas model for steam as the working fluid. For numerical simulation of flow field inside ejectors, it would be beneficial to study the effect of different numerical models on the accuracy of the numerical results. Such studies can be found in the researches published by Bartosiewicz et al. [18] on the effect of turbulence models and Cai and He [19] on the effect of ideal/real gas models. Other than entrainment ration, the compression ratio of an ejector could be used as the optimization criterion. In this regard, Sathiyamoorthy et al. [20] optimized an axial-axial flow ejector geometry for maximum compression ratio of the secondary flow. Many of the above references used ideal gas model and even incompressible flow conditions in their

simulations. In the current study, the real gas condition is considered in the simulations. This study is quite applied and it focuses on a special ejector with specific working conditions; however, the working condition can be improved suitably to improve the performance of ejector, which can subsequently improve the performance of upper-side ACC.

2. The Governing Equations

The flow field inside the ejector is turbulent. Also, because of very high working pressure of the primary flow which is going to be expanded and turn to high velocity through the motive nozzle, compressibility effects play crucial role. Besides, there are at least two species including water and air in the solution domain and the water component may go under phase change due to variation of temperature and pressure fields. Therefore, transport equations between the two species and the two phases (gas and liquid) should be taken into account. The governing equations for this problem then include conservation equations, transport of turbulence parameters, mixture and interphase transport equations and the equation of state. Conservation equations of mass, momentum and energy are given in Eqs. (1)-(3) in turbulent form as follows:

$$\frac{\partial}{\partial x_i}(\overline{\rho\, V_i}) + \frac{\partial}{\partial x_i}\left(\overline{\rho'\, V_i'}\right) = 0 \tag{1}$$

$$\rho\left[\frac{\partial \bar{V}_i}{\partial t} + \bar{V}_j \frac{\partial \bar{V}_i}{\partial x_j}\right] = \bar{B}_i - \frac{\partial \bar{P}}{\partial x_i} + \frac{\partial}{\partial x_j}\left[\mu \frac{\partial \bar{V}_i}{\partial t} - \rho\overline{V_i' V_j'}\right] \tag{2}$$

$$\rho\, C_p\, (\frac{\partial T}{\partial t} + \; V_j \frac{\partial T}{\partial x_j}) = \frac{\partial}{\partial x_j}\,(\mathrm{k}\frac{\partial T}{\partial x_j} - \rho\, C_p \overline{\acute{V}_j \acute{T}}\,) \tag{3}$$

The transport equations of turbulent kinetic energy (k) and dissipation rate of turbulent energy (ε) in RNG $k-\varepsilon$ turbulence model are also given in Eqs. (4) and (5), respectively. In Eq. (4), α_k is inverse effective Prandtl number for k parameter. In the right-hand-side of this equation, G_k, G_b, Y_M and S_k are generation of k due to mean velocity gradient, generation of k due to buoyancy, contribution of the fluctuating dilatation in compressible turbulence to the overall ε and k source term, respectively. Similarly, in Eq. (5), α_ε represents inverse effective Prandtl number for dissipation rate of turbulent energy. In the right-hand-side of this equation, $C_{1\varepsilon}, C_{2\varepsilon}$ and $C_{2\varepsilon}$ are constants, and R_ε and S_ε are specific terms in the RNG model and source term corresponds to the dissipation rate of turbulent energy, respectively.

$$\frac{\partial}{\partial t}(\rho k) + \frac{\partial}{\partial x_i}(\rho k V_i) = \frac{\partial}{\partial x_j}\left(\alpha_k \mu_{eff} \frac{\partial k}{\partial x_j}\right) + G_K + G_b + \rho\varepsilon + Y_M + S_k \tag{4}$$

$$\frac{\partial}{\partial t}(\rho\varepsilon) + \frac{\partial}{\partial x_i}(\rho\varepsilon V_i) = \frac{\partial}{\partial x_j}\left(\alpha_\varepsilon \mu_{eff} \frac{\partial \varepsilon}{\partial x_j}\right) + C_{1\varepsilon}\frac{\varepsilon}{k}(G_k + C_{3\varepsilon}G_b) - C_{2\varepsilon}\rho\frac{\varepsilon^2}{k} - R_\varepsilon + S_\varepsilon \tag{5}$$

For calculating some thermodynamic properties of the mixture inside the ejector, mass-weighed averaging method has been implemented. For example, the thermal conductivity of the mixture is to be simply calculated by Eq. (6). An identical method is used to calculate the constant pressure specific heat capacity of the mixture (Eq. (7)), while the heat capacities of each component are assumed to be polynomial functions of temperature.

$$k_m = \sum_i Y_i k_i \tag{6}$$

$$c_{p,m} = \sum_i Y_i c_{p,i} \tag{7}$$

Similar approach used for mixture dynamic viscosity in Eq. (8) by taking advantage of the well-known relation of Sutherland (Eq. (9)) to calculate the temperature-dependent viscosity of each species.

$$\mu_m = \sum_i Y_i \mu_i \tag{8}$$

$$\mu = \mu_0 \left(\frac{T_0 + T_{eff}}{T + T_{eff}}\right)\left(\frac{T}{T_0}\right)^{1.5} \tag{9}$$

In a mixture, two properties defined for species including mass and thermal diffusion. Mass diffusion is expressed in for of Fick's law in Eq. (10), in which D is constant mass diffusion coefficient. It means that all the species in the mixture diffuse their masses in similar manner. In this equation, J and ϕ are diffusive flux vector and molar concentration vector of the species, respectively. From the kinetic theory, the thermal diffusion coefficient is defined according to Eq. (11).

$$J = -D\nabla\phi \tag{10}$$

$$D_{T,i} = -2.59 \times 10^{-7} T^{0.659} \left[\frac{MW_i^{0.511} X_i}{\sum_i MW_i^{0.511} X_i} - Y_i\right]\left[\frac{\sum_i MW_i^{0.511} X_i}{\sum_i MW_i^{0.489} X_i}\right] \tag{11}$$

Due to the necessity of using a real gas model for the equation of state, Aungier-Redlich-Kwong real gas model is implemented here. The corresponding equation is given as

$$P = \frac{RT}{\bar{V} - b + c} - \frac{\alpha}{\bar{V}^2 + \delta\bar{V} + \varepsilon} \tag{12}$$

3. Results and Discussion

In this section, it is to investigate the effect of changing operating conditions on the performance of the target ejector and to find a better working condition at its design point. General layout of the primary configuration chosen to replace the existing ejector was shown in Fig. 2. In Fig. 3, the implemented boundary conditions are shown. For both the motive and suction inlets, the values of stagnation pressure and temperature are fixed. The ejector wall is assumed to be adiabatic with no-slip condition. Assuming the ejector exit section with a zero-gradient boundary, the static pressure and temperature are given then. Due to the symmetric geometry of the ejector, the configuration can be simulated asymmetrically. Two check points are used to investigate the validity and reliability of current numerical simulations, i.e., comparing the numerical results, like pressure and Mach number, at the points with the existing experimental data [11]. It should be mentioned that the amount of entrainment ratio has been also used as a validation parameter for the implemented numerical approach.

Fig. 3: Schematic of the ejector geometry and its boundary conditions.

Computational solution domain and its boundary conditions should be chosen similar to the real operating condition of ejector as much as possible. As can be seen in Fig. 3, an extended duct is attached to the diffuser of the ejector. Using this duct is completely in accordance to the related standards of experimental test of ejectors [21]. In this regard, and considering the numerical investigations on the effect of the length of this exit duct on the results, an exit duct of length of 12 inches is attached to the outlet of diffuser for making the similarity between the current numerical simulations and standard experiments.

After considering the prerequisites requirements for the simulations and having the alternative geometrical configuration, the next step is to study the effect of the operating conditions, e.g. primary stream stagnation pressure and temperature and investigate the ejector off-design performance. The behaviours of the ejector suction flow rate and the entrainment ratio under variation of the suction pressure are depicted in Figs. 4 and 5 for different motive stream stagnation pressures. As can be seen, it is obvious that for a fixed motive pressure, both the suction flow rate and the entrainment ratio increase as the suction pressure increases and it helps to the suction process. In fact, the suction pressure could be raised due to the rise of steam condenser pressure (steam turbine back pressure) in hot weather conditions. Figure 4 shows two different behaviours for the suction flow rate with an increment in the suction pressure. For the low suction pressures, the suction flow rate decreases as the motive pressure increases. If the suction pressure goes beyond a certain limit (about 15 to 20 kPa in this case), the behaviour will totally reverse, and higher motive pressures yield higher suction flow rates. This dualistic behaviour is the consequence of a struggle between two opposite sides. First, when we increase the motive pressure, the primary nozzle moves toward an under-expanded operating condition and the discharged flow to the mixing chamber needs to be expanded further. Extreme expansion of the primary stream could block the passage area of the secondary flow into the ejector and decrease the suction flow rate. Second, the rise of suction pressure will facilitate the entrance of the secondary flow into the ejector. Depending on the strength of the two parties of this contention, the suction flow rate may increase or decrease by increasing the motive pressure at a fixed value of suction pressure. As mentioned before, by decreasing the ratio of the primary stream stagnation pressure to the ejector discharge pressure, the primary nozzle operation will change from under-expanded to over-expanded condition. This can be achieved by decreasing the motive pressure at a fixed discharge pressure as shown in Fig. 6, note the contours of Mach number. In addition to replacing the expansion waves downstream of the motive nozzle by the oblique shock waves, these contours show that by decreasing the motive pressure, the ejector loses its isentropic flow and a normal shock wave starts moving upstream inside the exit duct and diffuser. Because of the higher entrainment ratio of the ejector at lower motive pressures, it is better to use motive stream of lower pressure and vary the current valuable 17.3 bar (abs.) superheated steam, which is supplied from a boiler, which provides 10 bar (absolute) steam extracted from high pressure turbine stages. Doing this, the entrainment ratio reaches to more than 51% from that of 16% in the current in-service ejector. It reduces the annual water consumption of the vacuum system of steam turbine condenser by more than 3000 m^3.

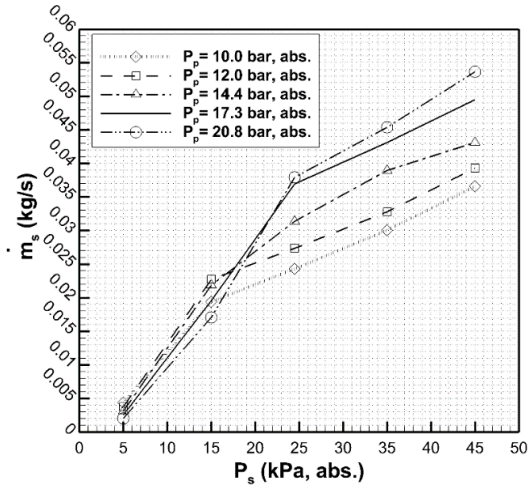

Fig. 4: Suction mass flow rate versus suction pressure at different motive stagnation pressures.

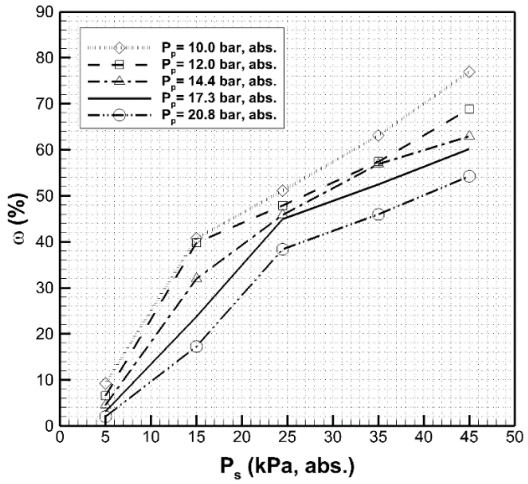

Fig. 5: Variation of ER with suction pressure at different motive stagnation pressures.

A steam ejector may work in off-design conditions because of two usual reasons. One reason is the variation in composition of the suction flow due to leakage of ambient air into the condenser heat exchangers. For the target ACC, the mass fraction of air inside the ejector suction flow at the design point is about 29%. The flow field inside ejector has been simulated with six different mass fractions of air in the secondary flow at five different suction pressures. Figure 7 shows the ejector entrainment ratio as a function of air mass fraction in the suction flow at different suction pressures. According to this figure, the mass fraction of air for each suction pressure has negligible effect on the entrainment ratio. This is because there are two forces, which act against each other. Since the molecular weight of air is greater than that of steam at the same pressure and temperature conditions, one unit volume of air-steam mixture with higher air mass fraction has greater mass than a unit volume containing lower amount of air. It should be mentioned that the absolute pressure of the motive stream at all the points in Fig. 7 is 17.3 bars.

The second off-design condition, which may happen in practice, is the raise in discharge ambient pressure due to the blockage of downstream inter/after condensers, piping, etc. The rise of ejector back pressure decreases the motive nozzle pressure ratio. As a result, a possible normal shock inside the exit duct or diffuser moves upstream and finally will be disappeared. This is shown in Fig. 8 via plotting the Mach contours. In order to quantify the discussion, one of the most important ejector performance curves, which shows the entrainment ratio versus the discharge pressure, is drawn in Fig. 9 for the current in-service ejector, the ejector after geometrical modifications, and the ejector after improving its operating conditions. As can be seen, the geometrical modifications only improve the entrainment ratio from 16 to 45% by maintaining the ejector critical back pressure near 110 kPa. The enhancement of the entrainment ratio continues with changing the operating conditions to more than 51%, while it causes the critical back pressure drops to near 50 kPa. It means that, it may be necessary to vary the motive stream pressure at off-design conditions and to move the ejector to a new operating point, which avoids malfunction of the ejector and reduction in its entrainment ratio.

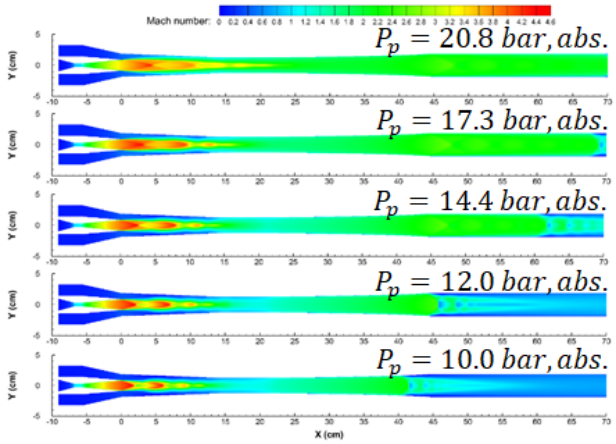

Fig. 6: Contours of Mach number at different motive stagnation pressures.

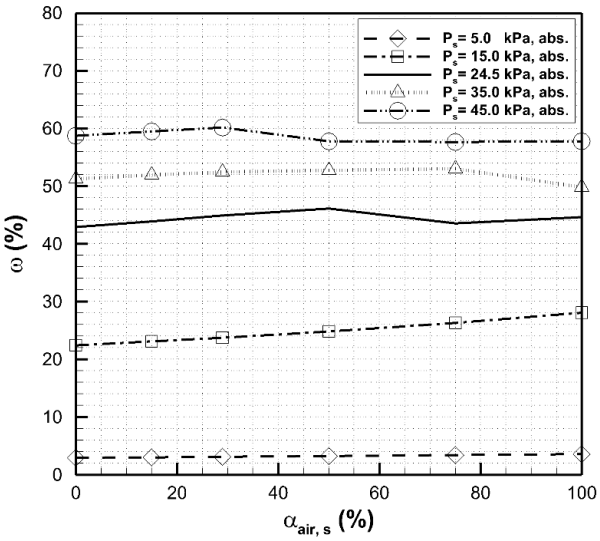

Fig. 7: Effect of air mass fraction in the suction stream on ER for different suction pressures.

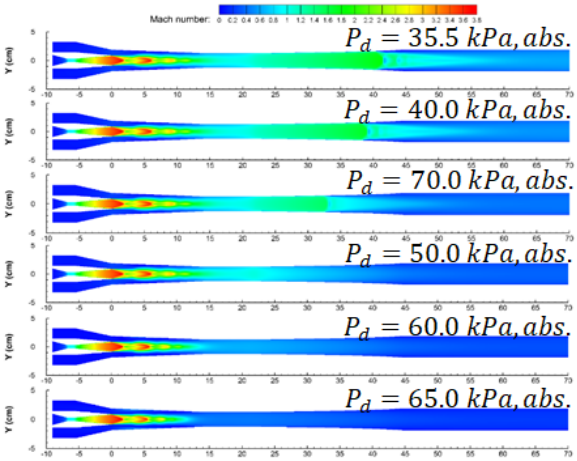

Fig. 8: Contours of Mach number inside the ejector for different amounts of discharge pressure.

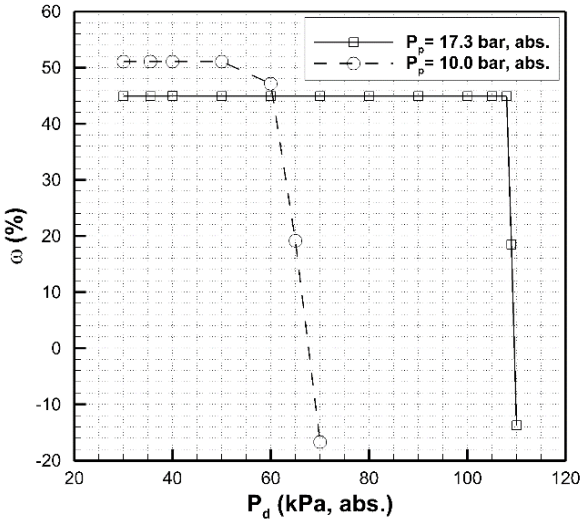

Fig. 9: Entrainment ratio as a function of discharge pressure at two different motive stream stagnation pressures.

4. Conclusion

In this work, we improved some real operating conditions for an in-use steam jet-ejector in a combined power cycle focusing on increasing its entrainment ratio. Extensive sets of numerical simulation were performed to investigate the effect of each operating condition on the ejector performance. By enhancing the entrainment ratio to more than 51%, the annual water consumption of the vacuum system can be reduced about 3000 m^3 in comparison with the existing in-service ejector. From the computational fluid dynamics aspect, it is concluded that a real gas model must be used for the equation of state to avoid underestimating the ejector entrainment ratio. It was found that by lowering the stagnation pressure of the motive stream, the entrainment ratio increases, while the ejector critical back pressure decreases. Hence, at off-design working conditions, it may be necessary to change the motive stream pressure and move the ejector to a new operating point in order to avoid the malfunction of ejector and reduction in its entrainment ratio. We also investigated the effects of mass fraction of air in the suction stream on the ejector performance. The results showed that this has an almost negligible effect on the amount of entrainment ratio at different suction pressure values.

Acknowledgements

The authors from Sharif University of Technology would like to thank the financial support received from the Deputy of Research and Technology in Sharif University of Technology. It is greatly acknowledged.

References

[1] X. C. Dai, G. J. Liao, "Numerical Simulation of Performance of Steam Ejector Influenced by the Distance between Nozzle Outlet and Mixing Chamber Inlet," *In Advanced Materials Research*, Trans Tech Publications, vol. 299, pp. 970-973, 2011.

[2] S. B. Riffat, G. Gan, S. Smith, "Computational fluid dynamics applied to ejector heat pumps," *Applied thermal engineering*, vol. 16, no. 4, pp. 291-297, 1996.

[3] H. Kim, Y. Lee, T. Setoguchi, S. Yu, "Numerical simulation of the supersonic flows in the second throat ejector-diffuser systems," *Journal of Thermal Science*, vol. 8, no. 4, p. 214, 1999.

[4] H. A. Al-Ansary, S. M. Jeter, "Numerical and experimental analysis of single-phase and two-phase flow in ejectors," *HVAC&R Research*, vol. 10, no. 4, pp. 521-538, 2004.

[5] K. Alhussan, C. Garris, "Effect of Changing Throat Diameter Ratio on a Steam Supersonic Pressure Exchange Ejector," *Modern Physics Letters B*, vol. 19, (28n29), pp. 1715-1718, 2005.

[6] Y. Zhu, W. Cai, C. Wen, Y. Li, "Numerical investigation of geometry parameters for design of high performance ejectors," *Applied Thermal Engineering*, vol. 29, no. 5, pp. 898-905, 2009.

[7] K. Ariafar, A. Toorani, "Effect of Nozzle Geometry on a Model Thermocompressor Performance–a Numerical Evaluation," *20th International Conference on Mechanical Engineering*, Shiraz University, Shiraz, Iran, 2012.
[8] S. Watanawanavet, " Optimization of a high-efficiency jet ejector by computational fluid dynamic software," Ph.D. Dissertation, Texas A&M University, 2005.
[9] K. Zhang, S. Shen, Y. Yang, "Numerical investigation on performance of the adjustable ejector," *International Journal of Low-Carbon Technologies*, ctq001, 2010.
[10] S. Varga, A. C. Oliveira, X. Ma, S. A. Omer, W. Zhang, S. B. Riffat, "Comparative Study Of The Performance Of A Variable Area Ratio Steam Ejector." *In 15th International Conference on Experimental Mechanics*, Porto/Portugal, pp. 22-27, 2012.
[11] W. Fu, Y. Li, Z. Liu, H. Wu, T. Wu, "Numerical study for the influences of primary nozzle on steam ejector performance," *Applied Thermal Engineering*, vol. 106, pp. 1148-1156, 2016.
[12] M. Palacz, J. Smolka, W. Kus, A. Fic, Z. Bulinski, A. J. Nowak, A. Hafner, "CFD-based shape optimisation of a CO 2 two-phase ejector mixing section," *Applied Thermal Engineering*, vol. 95, pp. 62-69, 2016.
[13] R. L. Yadav, A. W. Patwardhan, "Design aspects of ejectors: Effects of suction chamber geometry," *Chemical Engineering Science*, vol. 63, no. 15, pp. 3886-3897, 2008.
[14] T. Sriveerakul, S. Aphornratana, K. Chunnanond, "Performance prediction of steam ejector using computational fluid dynamics: Flow structure of a steam ejector influenced by operating pressures and geometries," *International Journal of Thermal Sciences*, vol. 46, no. 8, pp. 823-833, 2007.
[15] J. Chen, Z. Wang, J. Wu, W. Xu, "Investigation on the pressure matching performance of the constant area supersonic-supersonic ejector," *Thermal Science*, vol. 19, no. 2, pp. 631-643, 2015.
[16] M. Shafaee, M. Tavakol, R. Riazi, N. Sharifi, "An investigation on the supersonic ejectors working with mixture of air and steam," *Journal of Mechanical Science and Technology*, vol. 29, no. 11, pp. 4691-4699, 2015.
[17] H. Jeong, T. Utomo, M. Ji, Y. Lee, G. Lee, H. Chung, "CFD analysis of flow phenomena inside thermo vapor compressor influenced by operating conditions and converging duct angles," *Journal of mechanical science and technology*, vol. 23, no. 9, pp. 2366-2375, 2009.
[18] Y. Bartosiewicz, Z. Aidoun, Y. Mercadier, "Numerical assessment of ejector operation for refrigeration applications based on CFD," *Applied Thermal Engineering*, vol. 26, no. 5, pp. 604-612, 2006.
[19] L. Cai, M. He, "A numerical study on the supersonic steam ejector use in steam turbine system," *Mathematical Problems in Engineering*, 2013.
[20] K. Sathiyamoorthy, V. S. Iyengar, P. Manjunath, "Annular supersonic ejector design and optimization," *In ASME 2012 Gas Turbine India Conference*, American Society of Mechanical Engineers, pp. 85-93, 2012.
[21] Heat Exchanger Institute Inc., *HEI 2633: Standards for Steam Jet Vacuum Systems*, Ohio, 2000.